



# iMRI

Investigative  
Magnetic  
Resonance  
Imaging

## Original Article

Received: October 8, 2015  
Revised: November 22, 2015  
Accepted: November 23, 2015

### Correspondence to:

Seung Hong Choi, M.D., Ph.D.  
Department of Radiology, Seoul  
National University Hospital, 101  
Daehak-ro, Jongno-gu, Seoul  
110-744, Korea.  
Tel. +82-2-2072-2584  
Fax. +82-2-747-7418  
Email: verocay@snuh.org

This is an Open Access article distributed under the terms of the Creative Commons Attribution Non-Commercial License (<http://creativecommons.org/licenses/by-nc/3.0/>) which permits unrestricted non-commercial use, distribution, and reproduction in any medium, provided the original work is properly cited.

Copyright © 2015 Korean Society of Magnetic Resonance in Medicine (KSMRM)

# Application of Volumetric Analysis to Glioblastomas: a Correlation Study on the Status of the Isocitrate Dehydrogenase Mutation

Seon Yong Bae<sup>1</sup>, Chul-Kee Park<sup>2</sup>, Tae Min Kim<sup>3</sup>, Sung-Hye Park<sup>4</sup>, Il Han Kim<sup>5</sup>, Seung Hong Choi<sup>6,7,8,9</sup>

<sup>1</sup>Seoul National University College of Medicine, Seoul, Korea

<sup>2</sup>Department of Neurosurgery, Seoul National University Hospital, Seoul, Korea

<sup>3</sup>Department of Internal Medicine, Cancer Research Institute, Seoul National University Hospital, Seoul, Korea

<sup>4</sup>Department of Pathology, Seoul National University Hospital, Seoul, Korea

<sup>5</sup>Department of Radiation Oncology, Cancer Research Institute, Seoul National University Hospital, Seoul, Korea

<sup>6</sup>Institute of Radiation Medicine, Seoul National University Medical Research Center, Seoul, Korea

<sup>7</sup>Department of Radiology, Seoul National University Hospital, Seoul, Korea

<sup>8</sup>Center for Nanoparticle Research, Institute for Basic Science (IBS), Seoul, Korea

<sup>9</sup>School of Chemical and Biological Engineering, Seoul National University, Seoul, Korea

**Purpose:** To investigate whether volumetric analysis based on T2WI and contrast-enhanced (CE) T1WI can distinguish between isocitrate dehydrogenase-1 mutation-positive (IDH1<sup>P</sup>) and -negative (IDH1<sup>N</sup>) glioblastomas (GBMs).

**Materials and Methods:** We retrospectively enrolled 109 patients with histopathologically proven GBMs after surgery or stereotactic biopsy and preoperative MR imaging. We measured the whole-tumor volume in each patient using a semiautomatic segmentation method based on both T2WI and CE T1WI. We compared the tumor volumes between IDH1<sup>P</sup> (n = 12) and IDH1<sup>N</sup> (n = 97) GBMs using an unpaired t-test. In addition, we performed receiver operating characteristic (ROC) analysis for the differentiation of IDH1<sup>P</sup> and IDH1<sup>N</sup> GBMs using the tumor volumes based on T2WI and CE T1WI.

**Results:** The mean tumor volume based on T2WI was larger for IDH1<sup>P</sup> GBMs than IDH1<sup>N</sup> GBMs (108.8 ± 68.1 and 59.3 ± 37.3 mm<sup>3</sup>, respectively, P = 0.0002). In addition, IDH1<sup>P</sup> GBMs had a larger tumor volume on CE T1WI than did IDH1<sup>N</sup> tumors (49.00 ± 40.14 and 22.53 ± 17.51 mm<sup>3</sup>, respectively, P < 0.0001). ROC analysis revealed that the tumor volume based on T2WI could distinguish IDH1<sup>P</sup> from IDH1<sup>N</sup> with a cutoff value of 90.25 (P < 0.05): 7 of 12 IDH1<sup>P</sup> (58.3%) and 79 of 97 IDH1<sup>N</sup> (81.4%).

**Conclusion:** Volumetric analysis of T2WI and CE T1WI could enable IDH1<sup>P</sup> GBMs to be distinguished from IDH1<sup>N</sup> GBMs. We assumed that secondary GBMs with IDH1<sup>P</sup> underwent stepwise progression and were more infiltrative than those with IDH1<sup>N</sup>, which might have resulted in the differences in tumor volume.

**Keywords:** Glioblastoma; Isocitrate dehydrogenase (IDH); Magnetic resonance imaging (MRI)

## INTRODUCTION

Gliomas are the most prevalent primary neoplasm of the brain, and vary histopathologically from low grade to high grade (1). Malignant gliomas are categorized in the World Health Organization (WHO) system into four grades according to the presence of the following characteristics: atypia, mitoses, endothelial proliferation and necrosis (2). Secondary glioblastomas (GBMs) develop from WHO grade II or III gliomas, have a longer period of gliomagenesis, and arise from an early event such as an isocitrate dehydrogenase (IDH) gene mutation; however, primary GBMs occur *de novo* in older patients (3).

According to a recent genomic analysis of high-grade gliomas (HGGs), IDH gene mutations as a genetic marker of secondary GBMs matched the respective clinical diagnoses in 95% of cases (4). The IDH gene mutation has a direct relation with the role of abnormal metabolism in the pathogenesis and progression of these primary brain tumors (5). In fact, GBM patients with this mutation have a highly favorable prognosis, and IDH gene mutation testing is important for clinical patient management and stratification in clinical trials (4, 6–8).

Conventional MRI was used to analyze genetic alterations in GBMs in previous studies. Tumor texture analysis by T2 weighted image (WI) and contrast-enhanced (CE) T1WI can be used to predict the methylguanine methyltransferase (MGMT) promoter methylation status of GBM (9). The border characteristics and the homogeneity of the signal intensity of T2WI and T1WI can be used to assess the loss of 1p/19q (10). Additionally, the p53 mutation status and epidermal growth factor receptor (EGFR) status can be assessed by conventional MRI (11, 12).

To our knowledge, no previous study has used volumetric analysis based on T2WI and CE T1WI features to differentiate GBMs with and without IDH gene mutation. Thus, the purpose of this study was to identify the T2WI and CE T1WI features correlated with IDH gene mutation in GBMs.

## MATERIALS AND METHODS

Our Institutional Review Board approved this study, and the requirement for informed consent was waived.

### Patient Selection

One hundred and twenty-three patients who underwent

surgical resection or stereotactic biopsy at our institution between March 2008 and April 2014 were selected from our radiology report database. The inclusion criteria were as follows: (a) a histopathological diagnosis of GBM based on the WHO criteria (b) had undergone surgery or stereotactic biopsy and (c) had baseline MR imaging performed with T2WI and CE T1WI prior to the surgery or biopsy. We excluded 14 patients due to (a) poor-quality MR images and (b) to baseline MR imaging after the surgery. As a result, a total of 109 patients with GBM (69 males and 40 females; age range: 23–83 years; mean age: 56 years) were enrolled.

### Image Acquisition

For each patient, MR imaging was performed using a 3T scanner equipped with a 32-channel head coil (Verio; Siemens Healthcare Sector, Erlangen, Germany). The MR imaging included T1WI before and after contrast enhancement of the multi-planar reconstructed transverse and coronal imaging with a sagittal three-dimensional magnetization prepared rapid acquisition gradient echo (3D-MPRAGE) sequence, transverse fluid-attenuated inversion-recovery (FLAIR), and transverse T2WI with turbo spin-echo sequences. We obtained T1WIs with 3D-MPRAGE sequences using the following parameters: TR, 1500 ms; TE, 1.9 ms; flip angle (FA), 9°; matrix, 256 × 232; field of view (FOV), 220 × 250; section thickness, 1 mm; and number of excitations (NEX), 1. The parameters in the axial FLAIR imaging were a TR of 9000 ms, a TE of 97 ms, an inversion time of 2500 ms, a FA of 130°, a matrix of 384 × 348, a FOV of 199 × 220, and a slice thickness of 5 mm. The parameters in the transverse T2WI were as follows: TR, 5160 ms; TE, 91 ms; FA, 130°; matrix, 640 × 510–580; FOV, 175–199 × 220; section thickness, 5 mm; and NEX, 3. CE T1WI was obtained after intravenous administration of Gadobutrol (Gadovist®, Bayer Schering Pharma, Berlin, Germany) at a dose of 0.1 mmol per kilogram (mmol/kg) body weight.

### Quantitative Image Analysis

The MR imaging data were first transferred from the picture archiving and communication system workstation to a personal computer for further analyses. Image analysis was performed by an investigator (B.S.Y.) who was supervised by an expert neuroradiologist (C.S.H., 10 years of experience in neuroradiology). Coregistrations between the T2WI and CE T1WI were performed using a dedicated software package (NordicICE; NordicNeuroLab AS, Bergen, Norway), and semiautomatic segmentation was performed using another dedicated software package (NordicTumorEx).

The volume of interest (VOI) was defined by adjusting the elliptical VOI manually in the software, and automatic segmentation was considered within only the defined VOI. Observers were required to define a contrast-enhanced mass that avoided the cystic or necrotic regions, intralesional macrovessels, or perilesional edema on the CE T1WI and a higher signal intensity area than the grey matter on the T2WI. In terms of T2WI-based volumetrics, cystic or necrotic portions were included. The volume of each area was also presented because the analysis was performed using volume data derived from three-dimensional analysis. Automatic segmentation with clustering analysis was performed after determining the VOI. The clustering analysis was conducted using the Expectation and Maximization algorithm. The software presented three to seven clusters that did not overlap with one another in the segmented VOI. We chose a seven-cluster module within the segmented VOI, and the observers selected several clusters by visual inspection. The volume information for each tumor based on both the T2WI and CE T1WI was automatically calculated within the segmented VOI for every tumor.

**Statistical Analysis**

All statistical analyses were performed using the MedCalc software (MedCalc version 14.12.0; MedCalc Software, Mariakerke, Belgium). Results with a P value of less than 0.05 were considered statistically significant. The clinical characteristics were compared between the IDH1<sup>P</sup> and IDH1<sup>N</sup> groups using Fisher's exact test for categorical variables and an unpaired Student's t-test for non-categorical variables.

Kolmogorov-Smirnov's test was used to determine the normality of the distribution of non-categorical variables. According to the results of Kolmogorov-Smirnov's test, an unpaired Student's t-test was performed to compare tumor volume between the IDH1<sup>P</sup> and IDH1<sup>N</sup> groups. The area under the receiver operating characteristic (ROC) curve

(AUC) was used to determine the optimum tumor volume cutoff values for differentiating IDH1<sup>P</sup> from IDH1<sup>N</sup> using the method proposed by DeLong et al. (13). After obtaining cutoff values, sensitivities (detection of IDH1<sup>P</sup> GBM) and specificities (detection of IDH1<sup>N</sup> GBM) were calculated, and the ROC curves based on the tumor extents by T2WI and CE T1WI were compared between the two groups.

**RESULTS**

**Clinical Characteristics**

In the present study, we enrolled a total of 109 patients diagnosed with GBM: IDH1<sup>P</sup> (n = 12) and IDH1<sup>N</sup> (n = 97). No IDH2 mutation was detected in any of the patients. Among the clinical characteristics, only patient age was significantly lower in the IDH1<sup>P</sup> group compared to the IDH1<sup>N</sup> group (Table 1).

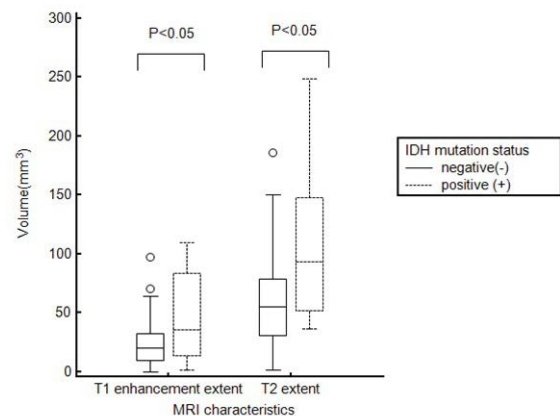


**Fig. 1.** Differences in tumor volume by CE T1WI and T2WI between the IDH1<sup>P</sup> and IDH1<sup>N</sup> groups. Box and plot graph showing means (line in box) and interquartile ranges of tumor volumes in the IDH1<sup>P</sup> and IDH1<sup>N</sup> groups. ○ = outliers.

**Table 1. Clinical Characteristics of the Patients**

Characteristics	Total	IDH1 <sup>P</sup>	IDH1 <sup>N</sup>	P value
Total number of patients	109	12	97	
Age, years	55.8 ± 13.9	40.8 ± 9.0	57.7 ± 13.2	0.0000421
Sex				1
Male	69	8	61	
Fmale	40	4	36	

Data are shown as means ± standard deviations.

IDH1<sup>N</sup> = negative for isocitrate dehydrogenase-1 mutation; IDH1<sup>P</sup> = positive for isocitrate dehydrogenase-1 mutation

### Volumetric Analysis Based on T2WI and CE T1WI

The mean tumor volume by CE T1WI was significantly larger in the IDH1<sup>P</sup> group than in the IDH1<sup>N</sup> group (49.0 ± 40.1 [mean ± standard deviation] mm<sup>3</sup> and 22.5 ± 17.5 mm<sup>3</sup>, respectively, P < 0.0001). The maximum value in the IDH1<sup>P</sup> group was 109.7 mm<sup>3</sup> and the minimum was 1.4 mm<sup>3</sup>. The maximum value in the IDH1<sup>N</sup> group was 97.9 mm<sup>3</sup> and the minimum was 0.4 mm<sup>3</sup> (Fig. 1).

Moreover, the IDH1<sup>P</sup> group showed a significantly larger volume by T2WI than the IDH1<sup>N</sup> group (108.8 ± 68.1mm<sup>3</sup> and 59.3 ± 37.3 mm<sup>3</sup>, respectively, P = 0.0002). The maximum value in the IDH1<sup>P</sup> group was 248.7 mm<sup>3</sup> and the minimum was 36.4 mm<sup>3</sup>. The maximum value in the IDH1<sup>N</sup> group was 185.9 mm<sup>3</sup> and the minimum was 1.8 mm<sup>3</sup> (Fig. 1). Figures 2 and 3 show representative cases of GBMs with IDH1<sup>P</sup> and IDH1<sup>N</sup>, respectively.

The CE T1WI to T2WI tumor volume ratio was not significantly different between the IDH1<sup>P</sup> and IDH1<sup>N</sup> groups (40.7 ± 25.5% and 43.1 ± 30.1%, respectively, P = 0.7925).

### Diagnostic Performance of Volumetric Analysis for the Differentiation of IDH1<sup>P</sup> from IDH1<sup>N</sup>

Table 2 summarizes the results of the ROC analyses

of mean tumor volume for the differentiation of IDH1<sup>P</sup> (n = 12) from IDH1<sup>N</sup> (n = 97) GBMs. The AUC values of the T1 enhancement and T2 extent of the tumors were 0.686 (0.590–0.771) and 0.733 (0.640–0.813), respectively (P = 0.0666 and 0.0035, respectively). In terms of the differentiation of IDH1<sup>P</sup> GBMs from IDH1<sup>N</sup> tumors, the sensitivity and specificity were 58.3% (7 of 12 IDH1<sup>P</sup>) and 81.4% (79 of 97 IDH1<sup>N</sup>), respectively, using a T2WI-based tumor volume cutoff value of 90.25 mm<sup>3</sup>.

### DISCUSSION

In this study of the imaging features of IDH1<sup>P</sup> and IDH1<sup>N</sup> GBMs on T2WI and CE T1WI, we found that IDH1<sup>P</sup> GBMs had a larger volume on both T2WI and CE T1WI, and the tumor extent on T2WI was more significantly different.

IDH mutation is a highly selective molecular marker of secondary GBMs that complements the clinical criteria for their differentiation from primary GBMs (7). Only ~5% of primary GBMs have IDH mutations; however, ~60–80% of diffusely infiltrating gliomas and secondary GBMs have IDH mutations (3, 5, 7). The IDH mutation state

**Table 2. Conventional Imaging for the Differentiation of IDH1<sup>P</sup> from IDH1<sup>N</sup>**

	AUC, median (95% CI)	Sensitivity (%)	Specificity (%)	Cutoff value	P value
T1 enhancement extent	0.686 (0.590–0.771)	50 (6 of 12 pts)	89.7 (87 of 97 pts)	> 44.97	0.0666
T2 extent	0.733 (0.640–0.813)	58.3 (7 of 12 pts)	81.4 (79 of 97 pts)	> 90.25	0.0035

Unless otherwise indicated, data in parentheses are 95% confidence intervals.

AUC = area under the receiver operator characteristic curve; CI = confidence interval; IDH1<sup>N</sup> = negative for isocitrate dehydrogenase-1 mutation; IDH1<sup>P</sup> = positive for isocitrate dehydrogenase-1 mutation; pts = patients

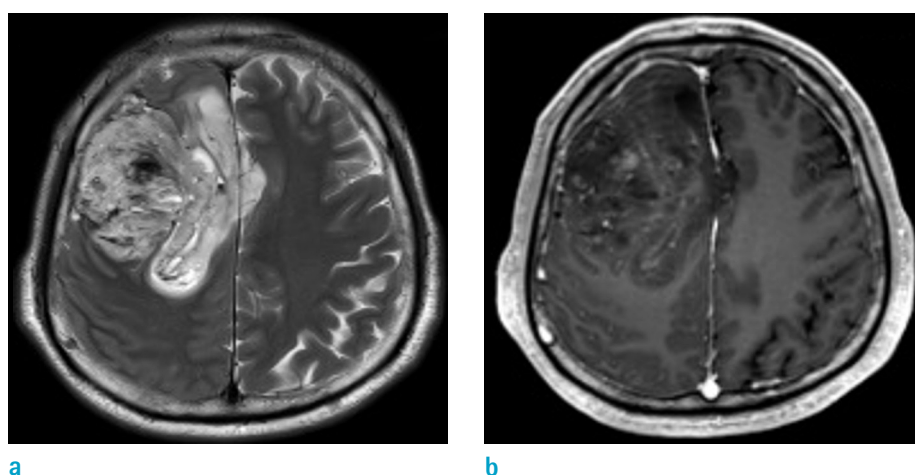


**Fig. 2.** Patient diagnosed with IDH1<sup>P</sup> GBM. A GBM with a high T2 signal intensity is observed in the right frontal lobe (a), which shows heterogeneous enhancement on CE T1WI (b).

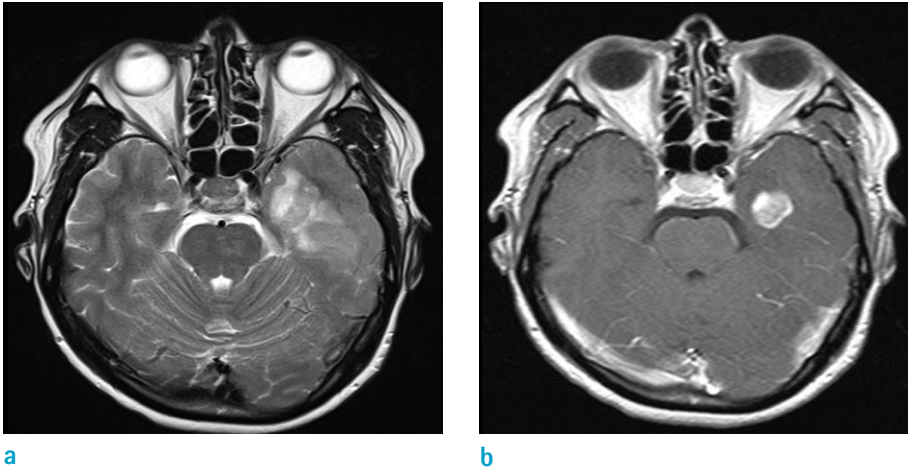


**Fig. 3.** Patient diagnosed with IDH1<sup>N</sup> GBM. A GBM with a high T2 signal intensity is observed in the left temporal lobe (a), which shows focal enhancement on CE T1WI (b). IDH1<sup>N</sup> GBMs tend to be smaller than IDH1<sup>P</sup> tumors by both T2WI and CE T1WI.

of these tumors is the cause of their different features. Secondary GBMs grow stepwise, and they infiltrate into other tissues; thus, their MR imaging and histopathological findings are heterogeneous, and the tumor is larger than primary GBMs (14–16). In addition, previous studies using magnetic resonance spectroscopy (MRS) showed that the accumulation of 2-hydroxyglutarate (2-HG) in the tumor was associated with IDH mutations in 30 patients with gliomas, which was likely related to the slow tumorigenesis of secondary GBMs (17–19).

To our knowledge, no study of the correlation of tumor volume imaging and the IDH mutation status has been performed, and few studies have assessed the therapeutic responses of GBM with IDH1 mutation using T2WI and CE T1WI (20, 21). Although several advanced MR imaging techniques, including perfusion study and diffusion-weighted imaging, have become popular for glioma evaluation (14), T2WI and CE T1WI remain essential for obtaining basic information such as tumor location and the extent and presence of leptomeningeal seeding, which are necessary for treatment planning. Our results suggest that by both T2WI and CE T1WI, the IDH1<sup>P</sup> group showed a significantly larger tumor volume than the IDH1<sup>N</sup> group. As mentioned above, secondary GBMs with the IDH1 mutation progress stepwise; thus, they have heterogeneous glioma components including low- and high-grade portions (14). Thus, we assumed that IDH1<sup>P</sup> GBMs could have a more infiltrative nature than IDH1<sup>N</sup> GBMs, which might cause differences in the tumor volumes on the T2WI and CE T1WI. Additionally, in a previous study (22), conventional MR imaging of GBM with IDH1<sup>P</sup> showed a large tumor size, the presence of large nonenhancing regions, and more frequent involvement of the frontal lobe. Interestingly, however, we

found no significant difference in the CE T1WI to T2WI tumor volume ratio between the two groups. We believe that the CE T1WI to T2WI tumor volume ratio of the GBMs could be affected more by tumor extent than by tumor heterogeneity, related to the IDH1 mutation status.

As mentioned above, relatively young patients were more frequent in the IDH1<sup>P</sup> group than in the IDH1<sup>N</sup> group (Table 1). It seems that the GBMs with IDH mutations start gliomagenesis earlier than those without IDH mutations. In previous reports (7, 23), there was also a marked difference in the age distribution of the patients with primary and secondary GBMs, and similarly those with and without IDH1 gene mutations.

Other than the intrinsic limits of any retrospective study, several other limitations to our work should be noted. First, the patient population was relatively small, and because of the retrospective nature of the study, there could have been selection bias due to the inclusion and exclusion criteria. Further investigation of a larger population is warranted. Second, the tumor boundary was defined with reference to T2WI. T2WI included either tumor infiltration or peritumoral edema or a combination of the two. However, it is impossible to differentiate between these two components in an image-based study. Third, we did not include advanced imaging techniques—such as MR spectroscopy, perfusion imaging and diffusion-weighted imaging—which can provide valuable information regarding glioma physiology and metabolism.

In conclusion, our results suggest that T2WI and CE T1WI analysis based on tumor volume can facilitate detection of the more infiltrative imaging features of IDH1<sup>P</sup> GBMs, which differ from those of IDH1<sup>N</sup> tumors. Conventional imaging of GBMs should be carefully assessed for an accurate diagnosis

and prognosis prediction.

### Acknowledgments

This study was supported by a grant from the Korea Healthcare technology R&D Projects, Ministry for Health, Welfare & Family Affairs (HI13C0015), Project Code (IBS-R006-D1), and a Man Chung Han research grant from the Department of Radiology, Seoul National University Hospital. The authors have no conflicts of interest to disclose.

### REFERENCES

1. Daumas-Duport C, Scheithauer B, O'Fallon J, Kelly P. Grading of astrocytomas. A simple and reproducible method. *Cancer* 1988;62:2152-2165
2. Pedersen CL, Romner B. Current treatment of low grade astrocytoma: a review. *Clin Neurol Neurosurg* 2013;115:1-8
3. Balss J, Meyer J, Mueller W, Korshunov A, Hartmann C, von Deimling A. Analysis of the IDH1 codon 132 mutation in brain tumors. *Acta Neuropathol* 2008;116:597-602
4. Nobusawa S, Watanabe T, Kleihues P, Ohgaki H. IDH1 mutations as molecular signature and predictive factor of secondary glioblastomas. *Clin Cancer Res* 2009;15:6002-6007
5. Yan H, Parsons DW, Jin G, et al. IDH1 and IDH2 mutations in gliomas. *N Engl J Med* 2009;360:765-773
6. Hartmann C, Hentschel B, Wick W, et al. Patients with IDH1 wild type anaplastic astrocytomas exhibit worse prognosis than IDH1-mutated glioblastomas, and IDH1 mutation status accounts for the unfavorable prognostic effect of higher age: implications for classification of gliomas. *Acta Neuropathol* 2010;120:707-718
7. Parsons DW, Jones S, Zhang X, et al. An integrated genomic analysis of human glioblastoma multiforme. *Science* 2008;321:1807-1812
8. Sanson M, Marie Y, Paris S, et al. Isocitrate dehydrogenase 1 codon 132 mutation is an important prognostic biomarker in gliomas. *J Clin Oncol* 2009;27:4150-4154
9. Levner I, Drabycz S, Roldan G, De Robles P, Cairncross JG, Mitchell R. Predicting MGMT methylation status of glioblastomas from MRI texture. *Med Image Comput Assist Interv* 2009;12:522-530
10. Jenkinson MD, du Plessis DG, Smith TS, Joyce KA, Warnke PC, Walker C. Histological growth patterns and genotype in oligodendroglial tumours: correlation with MRI features. *Brain* 2006;129:1884-1891
11. Aghi M, Gaviani P, Henson JW, Batchelor TT, Louis DN, Barker FG 2nd. Magnetic resonance imaging characteristics predict epidermal growth factor receptor amplification status in glioblastoma. *Clin Cancer Res* 2005;11:8600-8605
12. Mut M, Turba UC, Botella AC, Baskurt E, Lopes MB, Shaffrey ME. Neuroimaging characteristics in subgroup of GBMs with p53 overexpression. *J Neuroimaging* 2007;17:168-174
13. DeLong ER, DeLong DM, Clarke-Pearson DL. Comparing the areas under two or more correlated receiver operating characteristic curves: a nonparametric approach. *Biometrics* 1988;44:837-845
14. Lee S, Choi SH, Ryoo I, et al. Evaluation of the micro-environmental heterogeneity in high-grade gliomas with IDH1/2 gene mutation using histogram analysis of diffusion-weighted imaging and dynamic-susceptibility contrast perfusion imaging. *J Neurooncol* 2015;121:141-150
15. Ohgaki H, Kleihues P. The definition of primary and secondary glioblastoma. *Clin Cancer Res* 2013;19:764-772
16. Paganetti PA, Caroni P, Schwab ME. Glioblastoma infiltration into central nervous system tissue *in vitro*: involvement of a metalloprotease. *J Cell Biol* 1988;107:2281-2291
17. Andronesi OC, Rapalino O, Gerstner E, et al. Detection of oncogenic IDH1 mutations using magnetic resonance spectroscopy of 2-hydroxyglutarate. *J Clin Invest* 2013;123:3659-3663
18. Pope WB, Prins RM, Albert Thomas M, et al. Non-invasive detection of 2-hydroxyglutarate and other metabolites in IDH1 mutant glioma patients using magnetic resonance spectroscopy. *J Neurooncol* 2012;107:197-205
19. Choi C, Ganji SK, DeBerardinis RJ, et al. 2-hydroxyglutarate detection by magnetic resonance spectroscopy in IDH-mutated patients with gliomas. *Nat Med* 2012;18:624-629
20. SongTao Q, Lei Y, Si G, et al. IDH mutations predict longer survival and response to temozolomide in secondary glioblastoma. *Cancer Sci* 2012;103:269-273
21. Tran AN, Lai A, Li S, et al. Increased sensitivity to radio-chemotherapy in IDH1 mutant glioblastoma as demonstrated by serial quantitative MR volumetry. *Neuro Oncol* 2014;16:414-420
22. Carrillo JA, Lai A, Nghiemphu PL, et al. Relationship between tumor enhancement, edema, IDH1 mutational status, MGMT promoter methylation, and survival in glioblastoma. *AJNR Am J Neuroradiol* 2012;33:1349-1355
23. Jiao Y, Killela PJ, Reitman ZJ, et al. Frequent ATRX, CIC, FUBP1 and IDH1 mutations refine the classification of malignant gliomas. *Oncotarget* 2012;3:709-722